Selective epoxidation of alkenes using highly active V-SBA-15 materials: microwave *vs.* conventional heating†

Maria Jose Jurado, Maria Dolores Gracia, Juan Manuel Campelo, Rafael Luque,* Jose Maria Marinas and Antonio Angel Romero*

V-SBA-15 materials prepared using a hydrothermal methodology were found to be highly active and selective in the oxidation of a range of alkanes under mild reaction conditions. The activities of the systems were compared under conventional and microwave heating. Microwave experiments demonstrated that the long times of reaction (12–24 h) required under conventional heating could be reduced to a few minutes (15–60) with improved activities and selectivities under similar reaction conditions.

Introduction

The discovery of the surfactant-templated periodic mesoporous silicas (PMS) in the 1990s paved the way to the utilisation of highly useful porous materials in a wide range of applications including (bio)adsorption,[1,2] separation,[1,3] (bio)catalysis,[2] drug delivery[1,4] and related medical applications.[5] The amorphous thin fragile walls of M41S materials that conferred a poor hydrothermal stability were predated by long-range ordered SBA-type materials presenting enhanced hydrothermal stabilities with more stable and thicker walls.[6] Among them, hexagonal SBA-15 type materials have been extensively synthesised and reported as catalysts and supports in a variety of applications.[7–9] In the particular case of catalysis, the isomorphous substitution of Si for other metals including Al,[10] Zr[11] and Ti[12] in Si-SBA-15 materials was needed in order to generate acid and/or redox catalytically active sites on the synthesised solids. Compared to these commonly employed metals, vanadium has rarely been employed for such purposes despite its interesting redox properties.[13]

Selective greener oxidation processes are currently in great demand[3a,13–15] to offer an alternative to conventional stoichiometric methodologies employing toxic reagents and harsh reaction conditions which generally lead to poor selectivities and atom economies. Microwaves combined with heterogeneous active, stable and reusable solid oxidant catalysts are one of the most promising strategies to face this challenge. Microwave-assisted protocols, increasingly trendy over the last decade, have been reported to increase yields and in some cases selectivities to target products, reducing in parallel the reaction times and energy consumption.[16] V containing materials have been investigated in many oxidation processes including the oxidation of aromatics[17] and alkanes.[13,18]

In this work, we report that the selective oxidation of a range of alkenes can efficiently be performed, under both conventional heating and microwave irradiation, using highly active, selective and stable V-SBA-15 materials, with the only similar work reported by Peña *et al.* and George *et al.* on V-MCM-41[18] and Selvam and Dapurkar[19] on V-MCM-48 materials. The effect of different vanadium precursors on the incorporation of V into the mesoporous structure was investigated as well as the corresponding effects on the catalytic performance of the materials in the epoxidation of alkenes.

Experimental

V-SBA-15 materials were synthesised using a methodology previously reported.[10] In brief, a solution containing 8 g Pluronic P123 in 300 mL HCl at pH 1.5 was stirred at room temperature for 2 h. Tetraethyl orthosilicate (TEOS) as silica source and the desired quantities of vanadium precursors (vanadium oxytriisopropoxide and ammonium metavanadate) were stirred for 24 h and then the solution was aged in an oven at 100 °C for 24 h. The final solid obtained was then filtered off and subsequently calcined to extract the template at 600 °C under N_2 (4 h) and air (4 h).

In this way, V-SBA-15 materials with Si/V ratios ranging from 40 to 10 were synthesised. Materials were denoted as V-*X*-O/M where V makes reference to V-SBA-15 materials, *X* is the theoretical Si/V ratio (40 : 10) in the synthesis gel and O/M stands for the initials of the vanadium precursor employed in the synthesis procedure (O = vanadium oxytriisopropoxide; M = ammonium metavanadate). Thus, the catalyst V-30-M is a V-SBA-15 material with an Si/V 30 ratio which has been prepared using ammonium metavanadate as precursor.

Materials characterisation

Mesoporous V-SBA-15 materials were characterised by means of several techniques including X-ray diffraction (XRD), N_2 physisorption, transmission electron microscopy (TEM), UV-Vis and X-ray photoelectron spectroscopy (XPS).

Textural properties were determined from the N_2 adsorption–desorption isotherms using a volumetric adsorption analyzer Micromeritics ASAP 2000. Samples were outgassed at 130 °C under vacuum ($p < 10^{-2}$ Pa) for 24 h and subsequently analysed.

Departamento de Química Orgánica, Universidad de Córdoba, Edificio Marie Curie, Ctra Nnal IV, Km 396, E-14014 Córdoba, Spain. E-mail: q62alsor@uco.es; Fax: +34 957 212066; Tel: +34 957 212065
† This paper is part of a *Journal of Materials Chemistry* theme issue on Green Materials. Guest editors: James Clark and Duncan Macquarrie.

This journal is © The Royal Society of Chemistry 2009

J. Mater. Chem., 2009, **19**, 8603–8609 | 8603

The linear part of the BET equation was utilised for the determination of the specific surface area. Pore size distribution (PSD) was calculated from the desorption branch of the N_2 physisorption isotherms and the Barret–Joyner–Halenda (BJH) formula. The cumulative mesopore volume V_{BJH} was obtained from the PSD curve.

The elemental analysis of the V-SBA-15 materials was carried out at the Laboratorio de Mineralogía Aplicada (IRICA) of the Universidad de Castilla La Mancha (UCLM) using X-ray fluorescence spectrometry (XRFS) on a sequential Philips Magix PRO, with a simple goniometer based on channel measurements, under Rh Kα radiation. Powdered samples were compressed into 40 mm disks and subsequently analysed using the semi IQ+ program.

X-Ray diffraction patterns were recorded on a Philips X'PERT MPD PW3040 using Cu Kα radiation ($\lambda = 1.5418$ Å) over a 2θ range from 0.5 to 6° (1° per min).

Transmission electron microscopy (TEM) micrographs were recorded on an FEI Tecnai G^2 fitted with a CCD camera for ease and speed of use. The resolution is around 0.4 nm. Samples were suspended in ethanol and directly deposited on a copper grid prior to analysis.

XPS measurements were performed in a ultra high vacuum (UHV) multipurpose surface analysis system (Specs™ model, Germany) operating at pressures <10^{-10} mbar using a conventional X-ray source (XR-50, Specs, Mg Kα, 1253.6 eV) in a "stop-and-go" mode to reduce potential damage due to sample irradiation. The survey and detailed V and O high-resolution spectra (pass energy 25 and 10 eV, step size 1 and 0.1 eV, respectively) were recorded at room temperature with a Phoibos 150-MCD energy analyser. Powdered samples were deposited on a sample holder using double-sided adhesive tape and subsequently evacuated under vacuum (<10^{-6} Torr) overnight. Eventually, the sample holder containing the degassed sample was transferred to the analysis chamber for XPS studies. Binding energies were referenced to the C1s line at 284.6 eV from adventitious carbon.[20] The curve deconvolution of the obtained XPS spectra was obtained using the Casa XPS program. V2p curve fitting was performed on the V3p$_{3/2}$ region due to the overlapping between the O1s and the V2p$_{1/2}$ regions.

Catalytic experiments

Conventional heating. A typical conventional heating experiment was performed in a Carousel Reaction Station™ (Radleys Discovery Technologies) as follows: 31.1 mmol cyclohexene (3.15 mL), 4.5 mmol tert-butylhydroperoxide (TBHP, 0.5 mL), 7.4 mL dichloromethane (DCM) and 0.05 g of catalyst were added to a 20 mL carousel tube and heated at 43 °C (actual temperature measured using a Ni–Cr metallic thermocouple inserted periodically into the reaction vessel). Samples were withdrawn periodically, filtered off and analysed using an HP5890 Series II Gas Chromatograph (60 mL min^{-1} N_2 carrier flow, 20 psi column top head pressure) fitted with a capillary HP-101 column (25 m × 0.2 mm × 0.2 μm) and a flame ionisation detector (FID).

Microwave irradiation. Microwave experiments were carried out in a CEM-DISCOVER model with PC control and monitored by sampling aliquots of reaction mixture that were subsequently analysed by GC/GC-MS. Experiments were conducted in a closed vessel (pressure controlled) under continuous stirring. The microwave method was generally power-controlled where the samples were irradiated with the maximum power output (300 W) and different temperatures (60–80 °C), measured by an infra-red probe, were achieved. A typical catalytic reaction under microwave irradiation was conducted as follows: 10.3 mmol cyclohexene (1 mL), 1.5 mmol TBHP (0.17 mL), 1 mL DCM and 0.02 g catalyst were placed into a tube and microwaved for 1 h using maximum power output (300 W).

Response factors of the reaction products were determined with respect to the corresponding starting material from GC analysis using known compounds in calibration mixtures of specified compositions.

Results and discussion

Textural properties of the V-SBA-15 are summarised in Table 1.

In general, materials exhibited high surface areas (>250 m^2 g^{-1}) and pore diameters within the mesoporous range (typically around 5 nm). Surface areas and pore volumes decreased, as expected, as a consequence of the deterioration of the mesoporous structure with an increase in V content in the systems. Interestingly, a remarkable increase in pore size was observed at high V content (Si/V 5 and lower, Table 1, entries 5 and 9) that indicates structural changes in the SBA-15 materials (Fig. 1b). XRD results also show the advanced deterioration of the hexagonal mesoporous structure at increasing quantities of V (Fig. 1), with the absence of the 100 diffraction line below $2\theta = 1$ for the V-10 materials. These observations point to the loss of the mesoporous SBA-15 hexagonal structure for materials with Si/V ratios ≤20. Nevertheless, no diffraction lines were found in the

Table 1 Textural properties [surface area (S_{BET}, m^2 g^{-1}), pore diameter (D_{BJH}, nm), pore volume (V_{BJH}, cm^3 g^{-1})] of V-SBA-15 materials

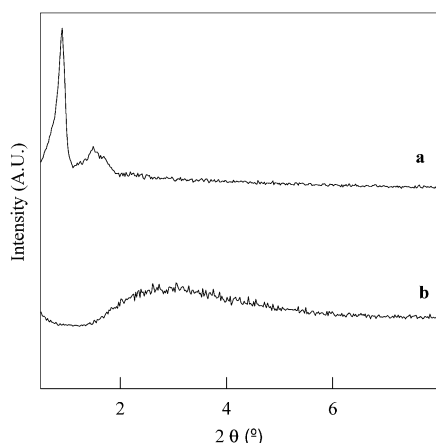| Entry	Material	S_{BET}/m^2 g^{-1}	D_{BJH}/nm	V_{BJH}/cm^3 g^{-1}	XRF (Si/V ratio)
1	Si-SBA-15	1016	5.7	1.15	—
2	V-40-O	931	5.1	0.71	42
3	V-30-O	810	4.6	0.47	44
4	V-20-O	592	5.2	0.66	13
5	V-10-O	373	9.3	0.38	5
6	V-40-M	1012	5.3	0.98	59
7	V-30-M	854	5.1	0.50	46
8	V-20-M	718	5.0	0.67	12
9	V-10-M	789	13.9	0.31	4

Fig. 1 XRD patterns of (a) Si-SBA-15 and (b) V-10-O.

20–80° range, which may indicate the absence of crystalline V_2O_5 domains in the materials.

In any case, the incorporation of V into the mesoporous structure was intriguing since the actual Si/V ratios were significantly different from those expected. Low loaded V-SBA-15 materials (Si/V 40 and 30) presented lower quantities of incorporated V in the calcined materials (Table 1, entries 3, 6 and 7). These findings may point to difficulties in the incorporation of V at low contents. In contrast to these results, increasing V contents (Si/V 20 and 10) lead to materials with remarkably superior Si/V
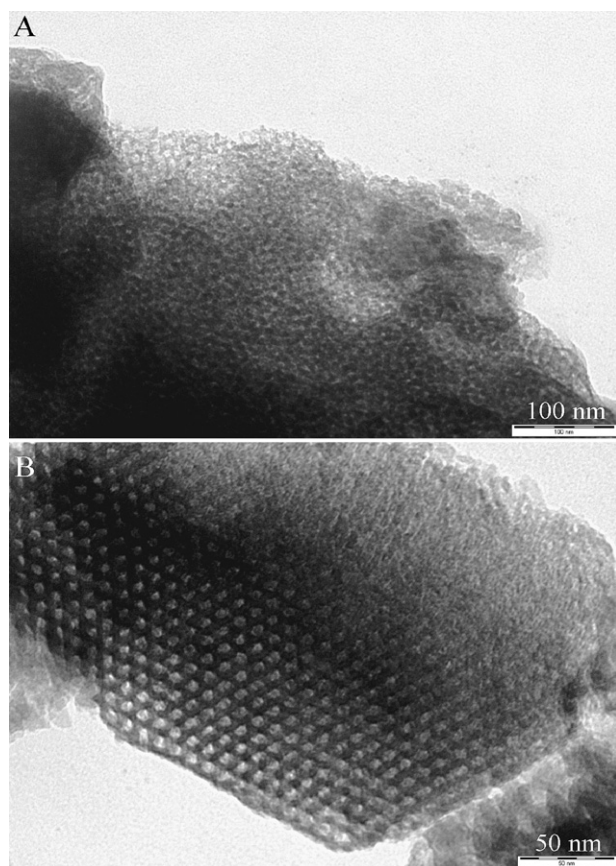
ratios to those theoretically expected from the synthesis gel (Table 1, entries 4, 5, 8 and 9). The metal is not homogeneously distributed within the mesoporous material at high V content due to the formation of high V concentration areas that will account for an inferior value of Si/V ratio in the XRF measurements.

The structural order of V-SBA-15 materials was confirmed by TEM. Fig. 2 clearly shows the hexagonal mesoporous channels with pores of *ca.* 5–6 nm for V-40-M (Fig. 2B), in good agreement with textural properties.

Isotherm profiles were typical of SBA-15 mesoporous materials (with a hysteresis loop in the desorption branch), although the deterioration of the structure was noticeable at increasing V contents (Fig. 3). The change in the isotherm profile for V-20 and V-10 materials together with the increasingly developed macroporosity (Fig. 3, p/p_0 values above 0.9) found for V-10 materials confirms the structural changes suggested in Table 1 and Fig. 1 that point to the loss of the mesoporous SBA-15 hexagonal order for high V content materials. This higher degree of macroporosity found for V-10 materials may account for the observed increase in pore diameter.

UV-Vis spectra are shown in Fig. 4. The profiles and intensity of the UV bands are independent of the V content in the materials and very broad bands were observed in general. A broad band in the 200–350 nm range (centred at *ca.* 250 nm) has been assigned to low energy ligand to metal charge transfer (LMCT) of tetrahedral V^{5+} species, coordinated to the SBA-15 surface,[18,21] suggesting the incorporation of V ions into the mesoporous structure.[18,19,21] Bands appearing in the 300–400 region (centred at *ca.* 400 nm) could be attributed to V–O–V (poly)/oligomeric species, with different degrees of oligomerisation, that have been previously reported in many vanadium materials.[22] Interestingly, the absence of UV absorption bands above 450 nm may point to the absence of significant quantities of V_2O_5 on the SBA-15 surface (LMCT transitions in V_2O_5 crystalline domains[18,19,22,23]). These findings were in good agreement with evidence found by XRD and XPS (Fig. 5 and 6).

XPS spectra of V-SBA-15 materials prepared with different vanadium precursors, including $V2p_{3/2}$ and $O1s$ regions, are presented in Fig. 5 and 6.
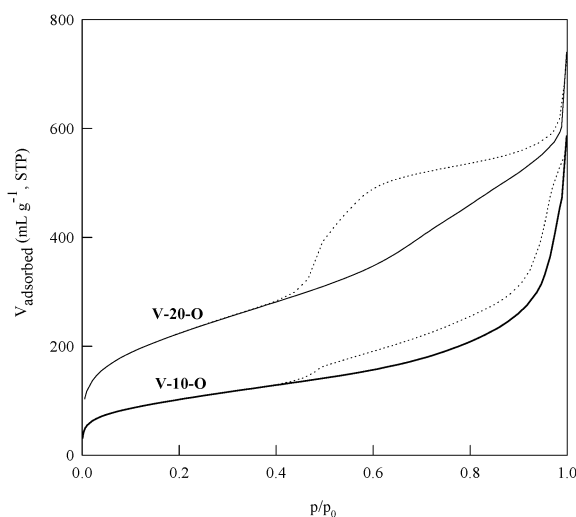

Fig. 2 TEM images of (A) V-10-O and (B) V-40-M.

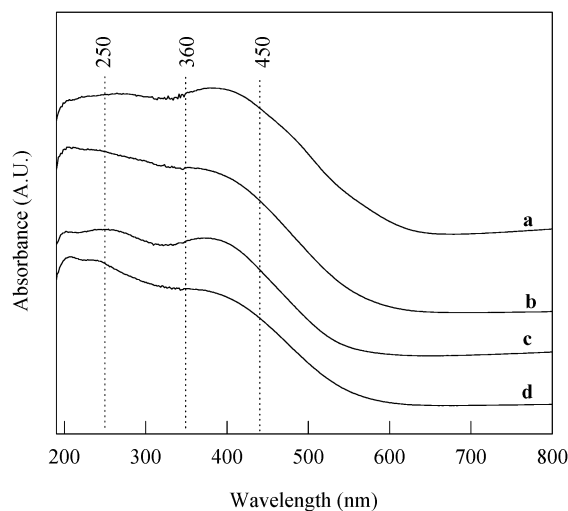**Fig. 3** Isotherm profiles of V-20-O and V-10-O materials.

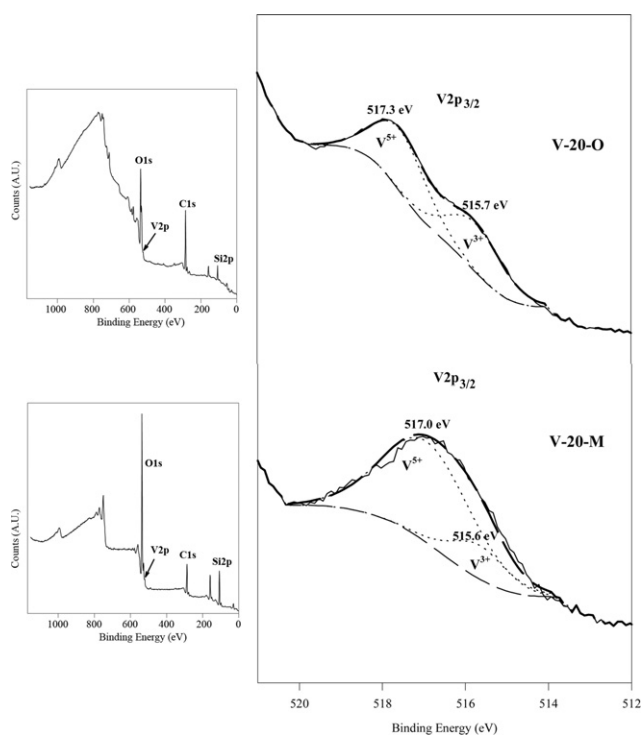**Fig. 4** UV-Vis spectra (190–800 nm) of V-SBA-15 materials: (a) V-10-M, (b) V-20-O, (c) V-30-M and (d) V-40-O.

Fig. 5 XPS spectra of V-20-O [survey (top-left) and V2p$_{3/2}$ (top-right)] and V-20-M [survey (bottom-left) and V2p$_{3/2}$ (bottom-right)].

V2p$_{3/2}$ bands centred at *ca.* 515.6 and 517.0 eV (main contribution) could be deconvoluted from the V2p$_{3/2}$ spectra. The 517.0 eV band, accounting for most of the V present in the materials, could be assigned to the V^{5+} oxidation state present within the mesoporous framework in tetrahedral coordination, in good agreement with previously reported results.[24] The component centred at *ca.* 515.6 eV (15% contribution) could similarly be assigned to V^{3+}, consistent with the energy shift observed for V^{5+}/V^{3+} species.[24,25] These results were also confirmed with the O1s XPS spectra that showed the three
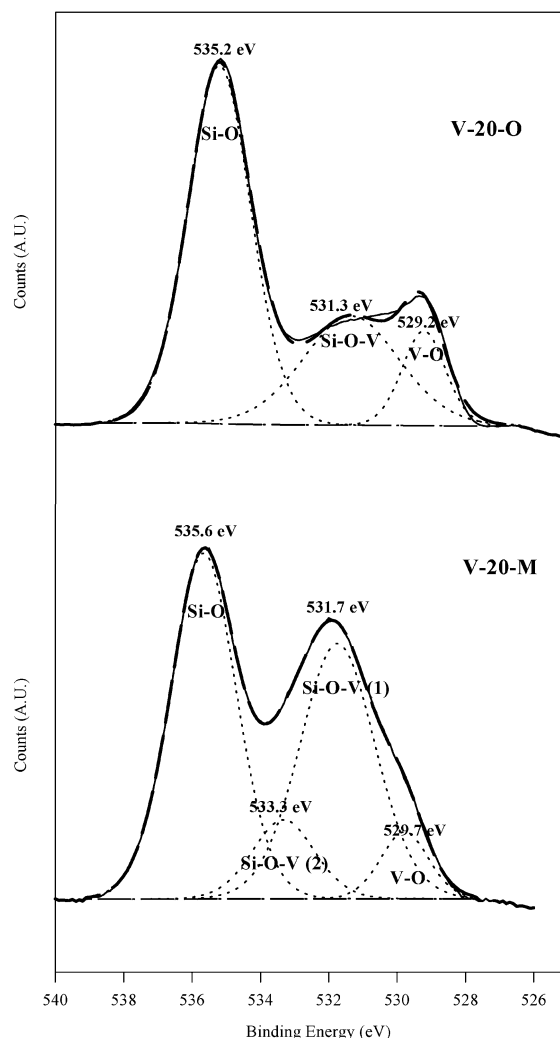

Fig. 6 O1s XPS spectra of V-20-O and V-20-M materials.

different O environments [2 from V (V–O from vanadium oxides and Si–O–V from vanadium framework) and the original Si–O from Si-SBA-15, Fig. 6].[26] These findings demonstrated that only minor quantities of vanadium oxides (V–O component, O1s band at *ca.* 529–530 eV in Fig. 6, <10% of total vanadium content) were observed in the materials, regardless of the vanadium precursor employed in their preparation, and also corroborate the successful incorporation of the majority of the V into the SBA-15 hexagonal mesostructure.

Interestingly, a new Si–O–V component could be clearly found in some of the materials [Si–O–V (2), Fig. 6, bottom]. These components have been reported to arise from the reversible coordination of water molecules to the pentavalent vanadium ions present in the tetrahedral framework structure, particularly that located near the pore entrance, which changes the coordination of V to octahedral.[19] It has been reported that these phenomena also cause a band broadening in UV-Vis spectra,[19] in good agreement with our UV-Vis results (Fig. 4).

Despite the low V$_2$O$_3$/V$_2$O$_5$ extra-framework content in the materials (<10%), interesting differences were observed for V-SBA-15 depending on the vanadium precursor utilised. The use of vanadium oxytriisopropoxide (V-*X*-O) rendered materials
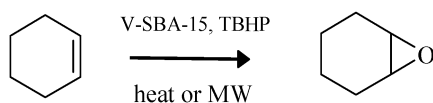
Scheme 1 Epoxidation of cyclohexene using V-SBA-15 materials under conventional heating or microwave irradiation.

with slightly higher vanadium extracted content (8–10%; *e.g.* vanadium oxides as suggested by V2p XPS spectra) than those found for V-M-O materials (<6%). These facts suggest that ammonium metavanadate may be a slightly better vanadium precursor for the V incorporation into the mesoporous structure than vanadium triisopropoxide.

The catalytic activity of V-SBA-15 materials was then investigated in the epoxidation of cyclohexene (Scheme 1) under conventional heating and microwave irradiation, and results were compared to demonstrate the efficiency of the microwave protocol.

Conventional heating experiments

Results are summarised in Fig. 7 and Table 2.

In general, the epoxidation reaction under conventional heating takes a long time (24 h+) to achieve good to quantitative conversion of starting material (97% conversion for V-20-O after
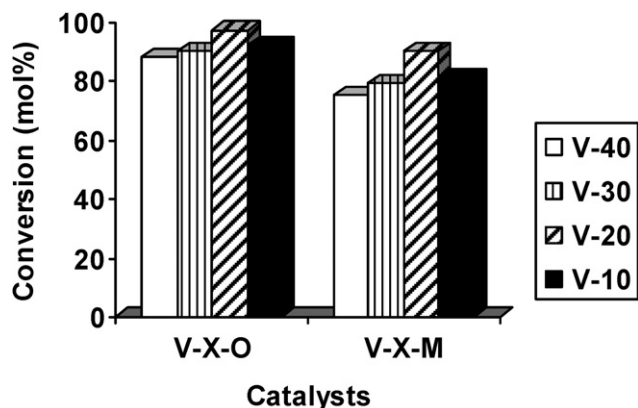

Fig. 7 Catalytic activity of V-*X*-O and V-*X*-M materials in the epoxidation of cyclohexene under conventional heating. *Reaction conditions*: 31.1 mmol cyclohexene, 4.5 mmol TBHP, 7.4 mL DCM, 0.05 g catalyst, 43 °C, 24 h.

Table 2 Catalytic activity of V-SBA-15 materials in the epoxidation of cyclohexene under conventional heating[a]

Material	Conversion (mol%)					TON	TOF/h^{-1}
	0.5 h	1 h	3 h	6 h	24 h		
V-40-O	32	45	60	72	88	780	32
V-30-O	32	44	65	75	90	820	34
V-20-O	45	62	77	86	97	300	12
V-10-O	42	46	66	76	92	140	6
V-40-M	23	34	48	58	75	900	38
V-30-M	23	38	53	64	79	700	29
V-20-M	39	53	68	76	90	270	11
V-10-M	21	34	45	58	81	120	5

[a] *Reaction conditions*: 31.1 mmol cyclohexene, 4.5 mmol TBHP, 7.4 mL DCM, 0.05 g catalyst, 43 °C.

24 h reaction, Table 2). Blank runs gave no cyclohexene conversion after 12 h reaction. Nevertheless, the catalysts were found to be extremely selective for the formation of cyclohexene oxide, with no other by-product(s) found under the investigated reaction conditions. Both V-20-O and V-20-M exhibited the highest conversions of starting material under the reaction conditions (Table 2). However, if we take into account the epoxidation activity per active site (supposedly from V species), TON and TOF values can provide a direct comparison between the investigated catalysts. Thus, despite their slightly inferior conversions, V-40 materials were found to be the most active catalysts in the epoxidation reaction, regardless of the vanadium precursor employed in their synthesis (Table 2). The significantly reduced activity observed for the V-10-Y materials can be attributed to the presence of high V concentration areas which have significantly reduced catalytic activities[27] as well as to the loss of hexagonal SBA-15 structure observed for these particular catalysts. Interestingly, the vanadium precursor did not seem to remarkably influence the activity of the materials. In general, V-*X*-O prepared with vanadium oxytriisopropoxide was only slightly more active compared to V-*X*-M prepared using ammonium metavanadate (Table 2). We believe the slightly superior quantities of extra-framework vanadium oxides (8–10% total V content) in V-*X*-O, as demonstrated by XPS, compared to V-*X*-M (5–6% maximum) may account for this little increase in activity observed for V-*X*-O.

Microwave experiments

Comparatively, the rates of reaction were significantly improved under microwave irradiation under similar conditions. Blank reactions (without catalyst) gave no conversion of starting material after 1 h reaction.

Results included in Fig. 8 point out that maximum conversions of 90% could be achieved with both V-20-O and V-20-M materials after 1 h of microwave irradiation compared to a poor 30–50% conversion reached under similar conditions, regardless of the catalyst employed in the epoxidation, under conventional heating (Table 2, 1 h column).
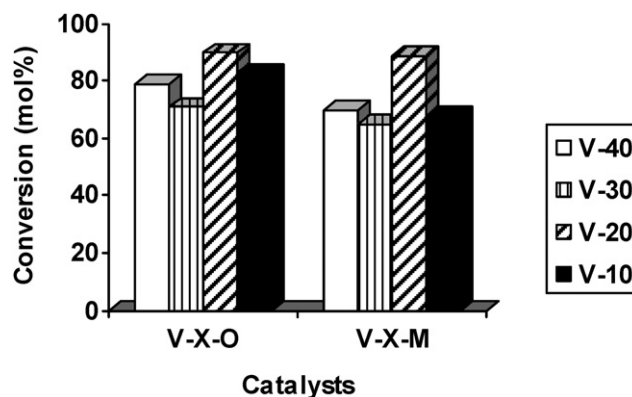

Fig. 8 Catalytic activity of V-*X*-O and V-*X*-M materials in the epoxidation of cyclohexene under microwave irradiation. *Reaction conditions*: 10.3 mmol cyclohexene, 1.5 mmol TBHP, 1 mL DCM, 0.02 g catalyst, 60–80 °C, 300 W, 1 h.
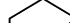
Table 3 Conventional heating *vs.* microwave irradiation. A comparison of activities for the most active catalyst V-40-M and V-40-O materials in the epoxidation of cyclohexene

Entry	Material	Method	Time of reaction/h [conversion value (mol%)]	TON	TOF/h^{-1}
1	V-40-O	Conventional heating[a]	24 [88]	780	32
2		Microwave irradiation[b]	1 [79]	570	570
3	V-40-M	Conventional heating[a]	24 [75]	900	38
4		Microwave irradiation[b]	1 [70]	700	700

[a] *Reaction conditions* (conventional heating): 31.1 mmol cyclohexene, 4.5 mmol TBHP, 7.4 mL DCM, 0.05 g catalyst, 43 °C, 24 h reaction. [b] *Reaction conditions* (microwave irradiation): 10.3 mmol cyclohexene, 1.5 mmol TBHP, 1 mL DCM, 0.02 g catalyst, 60–80 °C, 300 W, 1 h.

In any case, complete selectivities to cyclohexene oxide were observed in all systems, confirming the high selectivity of V-SBA-15 materials for the epoxidation reaction. Similar trends as those found in the conventional heating experiments were found for the activity in the systems with respect to Si/V ratio (V-20 materials as most active) and vanadium source (NH$_4$VO$_3$ as source gave less active materials) in the microwave experiments (Fig. 8).

Table 4 Comparison of activities between V-SBA-15 materials and other conventional oxidation catalysts in the epoxidation of cyclohexene to cyclohexene oxide under microwave irradiation[a]

Entry	Material	Conversion (mol%)	$S_{cyclohexene\ oxide}$ (%)
1	V-40-O	79	>99
2	V-20-O	90	>99
3	Ti-MCM-41	74	90
4	TiO$_2$	<10	>95
5[28]	Nb-PMOs[b]	16	85
6[15]	Co-salen-SBA-15[c]	75	80

[a] *Reaction conditions* (microwave irradiation): 10.3 mmol cyclohexene, 1.5 mmol TBHP, 1 mL DCM, 0.02 g catalyst, 300 W, 60–80 °C, 1 h. [b] *Reaction conditions*: 2 mmol cyclohexene, 2 mmol H$_2$O$_2$ (34 vol%), 0.04 g catalyst, 300 W, 45 °C, 1 h (ref. 28). [c] *Reaction conditions*: 20 mmol cyclohexene, 40 mmol H$_2$O$_2$ (34 vol%), 0.05 g catalyst, 300 W, 90 °C, 0.03 h (ref. 15).

Microwave *vs.* conventional heating

A further detailed comparison of the two most active catalysts (per V active site) under both conventional heating and microwave irradiation is included in Table 3. Turnover numbers (TONs) and turnover frequencies (TOFs, h^{-1}) clearly show the marked differences between the two protocols. While similar or even slightly superior TON values were achieved for conventional heating compared to microwave irradiation, TOF values were significantly reduced in conventional heating experiments (10–20 times inferior to those obtained under microwave irradiation) due to the long times of reaction required to achieve comparable conversion values. In any case, results demonstrate the superior performance of microwave-assisted protocols that are able to provide comparable conversions and selectivities (Table 3) to those obtained under conventional heating at remarkably reduced times of reaction (24 *vs.* 1 h, Table 3).

A comparison of the activity for the reported V catalysts with other conventionally employed epoxidation catalysts in the epoxidation of cyclohexene under microwave irradiation is also included in Table 4. Results clearly show the activities of V-SBA-15 materials were comparable and even superior, in most cases, to conventional TiO$_2$ and Ti-MCM-41 oxidation catalysts under identical reaction conditions. In any case, the complete selectivities observed in our systems (with not even traces of by-products under the investigated reaction conditions) are improved

Table 5 Catalytic activity of V-20-O in the epoxidation of a variety of cyclic and linear alkenes

Entry	Substrate	Method	Conversion (mol%)	Time of reaction/h	TON	TOF/h^{-1}
1		Conventional heating[a]	97	24	280	12
		Microwave irradiation[b]	89	1	230	230
2		Conventional heating[a]	95	24	300	12
		Microwave irradiation[b]	97	0.5	250	500
3		Conventional heating[a]	98	24	300	13
		Microwave irradiation[b]	94	0.25	250	1000
4		Conventional heating[a]	66	24	210	9
		Microwave irradiation[b]	77	1	200	200
5		Conventional heating[a]	74	24	230	10
		Microwave irradiation[b]	66	1	170	170

[a] *Reaction conditions* (conventional heating): 31.1 mmol alkene, 4.5 mmol TBHP, 7.4 mL DCM, 0.05 g V-20-O, 43–48 °C. [b] *Reaction conditions* (microwave irradiation): 10.3 mmol alkene, 1.5 mmol TBHP, 1 mL DCM, 0.02 g V-20-O, 60–80 °C, 300 W.

compared with those obtained in previous reports, highlighting the outstanding selectivities of this protocol. With regard to conventional heating processes, various reported results describe conversions ranging from 40 to 95% in 7–48 h, most of them are comparable to the catalytic activities obtained herein, with, however, much reduced selectivities to cyclohexene oxide (inferior to 90%).[29]

Investigation of the scope of the epoxidation reaction

Upon investigation of the activity of V-SBA-15 materials in the epoxidation of cyclohexene, the scope of the protocol was further extended to a range of alkenes as shown in Table 5 for both conventional heating and microwave irradiation using V-20-O as catalyst.

Blank reactions gave conversions inferior to 9% after 24 and 1 h reaction under conventional heating and microwave irradiation, respectively. Promisingly, the protocol was found to be amenable to both cyclic and linear alkenes, providing good to excellent conversions of starting material (e.g. 94% conversion of cyclooctene, >99% selectivity to the epoxide after 15 min microwave irradiation and a TOF of 1000 h^{-1}, Table 5, entry 3) with once again complete selectivities to the epoxidation product in all cases. An increase in TON and TOF values was observed with increasing the size of the ring containing the double bond (from cyclohexene to cyclooctene). Reduced activities were found for the particular case of less activated substrates (e.g. linear alkenes), with conversions around 70–80% and average TON values of 200 (Table 5, entries 4 and 5).

Most importantly, the active and stable mesoporous V-SBA-15 could be easily recovered and reused in the epoxidation reaction without significantly losing their initial activity after 3 cycles.

Conclusions

Mesoporous V-SBA-15 was synthesised using different vanadium precursors. Materials were found to be highly mesoporous, with developed macroporosity at increasing V contents in the solids. The catalytic activity of V-SBA-15 was subsequently investigated in the epoxidation of a range of cyclic and linear alkenes under both conventional heating and microwave irradiation. Results proved that the materials were very active and selective to the formation of the respective epoxides, with remarkably reduced times of reaction under microwave irradiation (0.25–1 h) compared to those needed under conventional heating (24 h+) to achieve comparable conversion values. Materials could be also recovered upon reaction completion and reused at least 3 times with almost complete preservation of the initial activity. We envisage our materials will be employed in many oxidation processes in the future and further research is already ongoing in our laboratories.

Acknowledgements

References

1 G. A. Ozin, A. Arsenault and L. Cademartiri, *Nanochemistry. A Chemical Approach to Nanomaterials*, RSC Publishing, Cambridge, UK, 2nd edn, 2009.

2 M. S. Rigutto, R. Van Veen and L. Huve, *Stud. Surf. Sci. Catal.*, 2007, **168**, 837–854.

3 (a) G. Rothenberg, *Catalysis. Concepts and Green Applications*, Wiley-VCH, Weinheim, Germany, 2008; (b) M. Hartmann, *Chem. Mater.*, 2005, **17**, 4577–4593.

4 M. Vallet-Regi, F. Balas and D. Arcos, *Angew. Chem., Int. Ed.*, 2007, **46**, 7548–7558.

5 M. Vallet-Regi, L. Ruiz-Gonzalez, I. Izquierdo-Barba and J. M. Gonzalez-Calbet, *J. Mater. Chem.*, 2006, **16**, 26–31.

6 (a) D. Zhao, Q. Huo, J. Feng, B. F. Chmelka and G. D. Stucky, *J. Am. Chem. Soc.*, 1998, **120**, 6024–6036; (b) D. Zhao, J. Feng, Q. Huo, N. Melosh, G. H. Frederickson, B. F. Chmelka and G. D. Stucky, *Science*, 1998, **279**, 548–552.

7 S. K. Badamali, R. Luque, J. H. Clark and S. W. Breeden, *Catal. Commun.*, 2009, **10**, 1010–1013.

8 (a) X. Liu, A. Wang, X. Wang, C. Y. Mou and T. Zhang, *Chem. Commun.*, 2008, 3187–3189; (b) Sujandi, E. A. Prasetjanto and S. E. Park, *Appl. Catal., A*, 2008, **350**, 244–251.

9 (a) Y. Li, H. Xia, F. Fan, Z. Feng, R. A. Van Santen, E. J. M. Hensen and C. Li, *Chem. Commun.*, 2008, 774–776; (b) H. Li, W. Chai, F. Zhang and J. Chen, *Green Chem.*, 2007, **9**, 1223–1228; (c) H. Liu, H. Wang, J. Shen, Y. Sun and Z. Liu, *Catal. Today*, 2008, **131**, 444–449.

10 M. J. Gracia, E. Losada, R. Luque, J. M. Campelo, D. Luna, J. M. Marinas and A. A. Romero, *Appl. Catal., A*, 2008, **349**, 148–155.

11 (a) F. Li., F. Yu, Y. Li, R. Li and K. Xie, *Microporous Mesoporous Mater.*, 2007, **101**, 250–255; (b) B. L. Newalkar, J. Olanrewaju and S. Komarneni, *J. Phys. Chem. B*, 2001, **105**, 8356–8360.

12 (a) J. Iglesias, J. A. Melero and J. Sainz-Pardo, *J. Mol. Catal. A: Chem.*, 2008, **291**, 43–53; (b) A. Vinu, P. Srinivasu, D. Miyahara and K. Ariga, *J. Phys. Chem. B*, 2006, **110**, 801–806.

13 G. J. Hutchings, *J. Mater. Chem.*, 2009, **19**, 1222–1235.

14 *Methods and Reagents for Green Chemistry*, ed. P. Tundo, A. Perosa and F. Zecchini, John Wiley & Sons, Hoboken, NJ, 2007.

15 R. Luque, S. K. Badamali, J. H. Clark, M. Fleming and D. J. Macquarrie, *Appl. Catal., A*, 2008, **341**, 154–159.

16 C. O. Kappe, *Chem. Soc. Rev.*, 2008, **37**, 1127–1139.

17 (a) F. M. Bautista, J. M. Campelo, D. Luna, J. Luque, J. M. Marinas and M. T. Siles, *Chem. Eng. J. (Amsterdam, Neth.)*, 2006, **120**, 3–9; (b) R. K. Jha, S. Shylesh, S. S. Bhoware and A. P. Singh, *Microporous Mesoporous Mater.*, 2006, **95**, 154–163.

18 (a) M. L. Peña, A. Dejoz, V. Fornés, F. Rey, M. I. Vazquez and J. M. Lopez-Nieto, *Appl. Catal., A*, 2001, **209**, 155–164; (b) J. George, S. Shylesh and A. P. Singh, *Appl. Catal., A*, 2005, **290**, 148–158.

19 P. Selvam and S. E. Dapurkar, *J. Catal.*, 2005, **229**, 64–71.

20 C. C. Chusuei, M. A. Brookshier and D. W. Goodman, *Langmuir*, 1999, **15**, 2806–2808.

21 (a) G. Xiong, C. Li, Q. Xin and Z. Feng, *Chem. Commun.*, 2000, 677–678; (b) C. Hess, J. D. Hoefelmeyer and T. D. Tilley, *J. Phys. Chem. B*, 2004, **108**, 9703–9709.

22 T. Tsoncheva, L. Ivanova, R. Dimitrova and J. Rosenholm, *J. Colloid Interface Sci.*, 2008, **321**, 342–349 and references therein.

23 H. Tian, E. I. Ross and I. E. Wachs, *J. Phys. Chem. B*, 2006, **110**, 9593–9600.

24 M. A. Eberhardt, A. Prcotor, M. Houalla and D. M. Hercules, *J. Catal.*, 1996, **160**, 27–34.

25 J. Nickl, Ch. Schild, A. Baiker, M. Hund and A. Woukam, *Fresenius' J. Anal. Chem.*, 1993, **346**, 79–83.

26 D. A. Pawlak, M. Ito, M. Oku, K. Shimamura and T. Fukuda, *J. Phys. Chem. B*, 2002, **106**, 504–507.

27 A. Baiker, P. Dollenmeier, M. Glinski, A. Reller and V. K. Sharma, *J. Catal.*, 1988, **111**, 273–285.

28 K. Walczak and I. Nowak, *Catal. Today*, 2009, **142**, 293–297.

29 (a) S. Mukerjee, S. Samanta, A. Bhaumik and B. C. Ray, *Appl. Catal., B*, 2006, **68**, 12–20; (b) E. M. Serwicka, J. Poltowicz, K. Bahranowski, Z. Olejniczak and W. Jones, *Appl. Catal., A*, 2004, **275**, 9–14; (c) O. A. Kholdeeva, T. A. Trubitsina, M. N. Timofeeva, G. M. Maksimov, R. I. Maksimovskaya and V. A. Rogov, *J. Mol. Catal. A: Chem.*, 2005, **232**, 173–178; (d) Sujandi, S. C. Han, D. S. Han, M. J. Jin and S. E. Park, *J. Catal.*, 2006, **243**, 410–419.